

Irradiation damage on CrNbTaVW_x high entropy alloys

R. Martins ^{a,*}, J.B. Correia ^b, P. Czarkowski ^c, R. Miklaszewski ^c, A. Malaquias ^a, R. Mateus ^a, E. Alves ^a, M. Dias ^a

^a Instituto de Plasmas e Fusão Nuclear, Instituto Superior Técnico, Universidade de Lisboa, Av. Rovisco Pais, 1049-001 Lisboa, Portugal

^b LNEG, Laboratório Nacional de Energia e Geologia, Estrada do Paço do Lumiar, 1649-038 Lisboa, Portugal

^c Institute of Plasma Physics and Laser Microfusion (IPPiLM), 23 Hery Str., 01-497 Warsaw, Poland



ARTICLE INFO

Keywords:

Plasma facing components
High entropy alloys
Irradiation damage
Melting
Swelling

ABSTRACT

CrNbTaVW_x high-entropy alloys have been developed for plasma facing components to be applied in nuclear fusion reactors. The CrNbTaVW_x ($x = 1$ and 1.7) compositions were prepared by ball milling and consolidated at $1600\text{ }^{\circ}\text{C}$ under 90 MPa . To study the irradiation resistance of these materials, deuterium plasmas were used to irradiate the samples in the PF-1000U facility with 1 and 3 discharges. Structural changes before and after irradiation were analyzed by scanning electron microscopy coupled with energy dispersive X-ray spectroscopy. Nuclear reaction analysis was carried out with 1000 and 2300 keV ${}^{3}\text{He}^{+}$ ion beams to evaluate the profile and amount of retained deuterium on the irradiated samples. After irradiation, the sample with higher W content revealed swelling and melting for all discharges, while in the case of CrNbTaVW only blisters were observed. The deuterium retention was higher for CrNbTaVW_{1.7} when compared with CrNbTaVW for 3 discharges applied.

1. Introduction

There is an urgent need to develop novel and advanced nuclear materials to guarantee that a future nuclear fusion reactor can operate continuously and safely, ensuring a long-life of the plasma facing components. Tungsten is the leading high atomic number candidate for plasma-facing components due to its high melting point, high sputtering threshold, corrosion resistance, and tensile strength [1–3]. However, one of the main drawbacks is high Ductile-to-Brittle Transition Temperature (DBTT) of tungsten, which should operate at $350\text{--}400\text{ }^{\circ}\text{C}$ [4].

The proposed strategy to increase the fracture toughness of W includes the development of high-entropy alloys HEAs through a powder metallurgy route [5,6]. In the last few years, this multi-component systems called HEAs attracted special attention for nuclear fusion applications. HEAs are solid solutions with simple BCC (body centered cubic), FCC, (face centered cubic) or HCP (hexagonal closed packed) crystal structures with five or more elements that range between 5 and 35 at. %, an equiatomic or non-equiatomic alloy has the same or different percentage in the number of atoms, with this HEAs have a unique set of promising properties such as high hardness [7], high thermal conductivities [8] as well as high thermal [9] and irradiation [3,10,11] resistance. The numerous combinations of the elements, the production processes available, the conditions, and the environment in

which the alloy will operate, were requirements remarkably difficult to achieve. There are some studies that demonstrated that HEAs exhibit a high fracture toughness such as $\text{Ti}_3\text{Zr}_{1.5}\text{NbVAl}_{0.25}$ alloy [12] which shows better combination between strength and toughness than most traditional alloys and HEAs. In addition, previous work on the present equiatomic (CrNbTaVW₁) and non-equiatomic HEAs (CrNbTaVW_{1.7}) [13] showed that the non-equiatomic alloy evidence an improvement of mechanical properties. Based on this result, it is believed that these materials have potential for the present application. However, irradiation resistance studies are necessary. For this purpose, a plasma focus machine was used that is capable to generate directed, dense hot plasma flows and fast ion streams with incident energies for light deuterium that can range from dozens of keV up to few MeV and can be suitable for fusion first wall studies. In the present experiment, HEAs were irradiated in the large Plasma Focus devices PF-1000U with deuterium plasmas. Scanning electron microscopy coupled with energy-dispersive X-ray spectroscopy will be used to characterize the surface of the irradiated materials. In addition, nuclear reaction analysis (NRA) will identify the depth profile and quantify the deuterium retention in the exposed surfaces.

* Corresponding author.

E-mail address: ricardo.martins@ctn.tecnico.ulisboa.pt (R. Martins).

Table 1

Element composition for equiatomic (CrNbTaVW) and non-equiatomic ($\text{CrNbTaVW}_{1.7}$) HEA.

Element	(at.%) in CrNbTaVW	(at.%) in $\text{CrNbTaVW}_{1.7}$
Cr	20	17.5
Nb	20	17.5
Ta	20	17.5
V	20	17.5
W	20	30

Table 2

Irradiation parameters in the PF-1000U device [15].

Background gas (66.7 Pa)	$^2\text{H}_2$ (100%)
Average power flux density of HP (P_{HP})*	$\sim 10^8 \text{ W/cm}^2$
Irradiation time of HP (t_{HP})*	$\sim 100 \text{ ns}$
Average power flux density of FIS (P_{FIS})*	$\sim 2.5 \times 10^9 \text{ W/cm}^2$
Irradiation time of FIS (t_{FIS})*	$\sim 40-50 \text{ ns}$
Average Ion Fluence	$\sim 7.5 \times 10^{15} \text{ ion/cm}^2$
Predicted maximum target temperature	$\sim 2773 \text{ K}$

2. Experimental details

Table 1 presents the element composition for W, Cr, Ta, Nb, and V powders (AlfaAesar, nominal purity of 99.9% with average particle size of 10 μm) that were mixed, in a glove box and mechanically alloyed in a high-energy planetary ball mill PM 400, with tungsten carbide balls and vials.

The balls to powder mass ratio was 10:1, and the milling was carried out at 380 rpm for 2 h. The consolidation of CrNbTaVW_x ($x = 1$ and 1.7) samples was performed in graphite dies of 10 mm diameter and 5 mm height by the Upgraded Field Assisted Sintering Technology (U-FAST) process.

A preliminary degassing step was conducted at 873 K for 2 min under a pressure of 15 MPa. The samples were then sealed under vacuum (5×10^{-3} Pa), at a temperature of 1873 K, and external hydrostatic pressure of 90 MPa was applied for 10 min and then allowed to cool to room temperature. The final discs produced have a volume of 0.63 cm^3 with an average weight of 6.86 g. After sintering, the apparent density was measured by the Archimedes method [14].

Metallographic preparation of the samples was performed by grinding with SiC paper and polishing with diamond suspensions (6 μm , 3 μm , and 1 μm) and finely polished with colloidal silica suspension (0.2 μm). A JEOL JSM-7001F field emission gun scanning electron microscope equipped with an Oxford energy dispersive X-ray spectroscopy (EDS) system was used to observe the microstructure prior to and after irradiation using secondary electron image (SE).

Polished CrNbTaVW_x ($x = 1$ and 1.7) samples were irradiated with deuterium plasma with 1, and 3 discharges using parameter shown in **Table 2** [15]. PF-1000U is a dense plasma focus device of the Institute of plasma Physics and Laser Microfusion (IFPiLM), Warsaw, Poland, that generates hot plasma (HP) and fast ions streams (FIS) discharges in the energy in the range 600–1000 kJ. Beyond the heat flows, typical particle fluences using deuterium as background are close to 7.5×10^{15} ions/ cm^2 . Most of the fast stream ions present an average incident energy close to 100 keV [16,17]. Most of the fast stream ions present an average incident energy close to 100 keV. At higher energies ion density presents an exponential decay up to 8–10 MeV. Thus, it is expected the retention of deuterium deeply inside the irradiated samples. Moreover, fuel retention measurements were performed with simultaneous Rutherford Backscattering Spectrometry (RBS) and NRA. Fitting the NRA yield values together with RBS allow us to obtain the depth profile that relates the RBS values obtained from each sample analyzed in five distinct zones,

and the depth that the deuterium is retained, creating a graph that gives us how much deuterium exists in each depth. The use of incident 1000 keV $^3\text{He}^+$ ion beams lead to enhanced sensitivity for deuterium quantification at the surface layers, and a depth limit of 3.3 μm for the analysis of the present HEA alloys is achieved with 2300 keV $^3\text{He}^+$ beams. In the present experiment, both incident energies were used. Each sample was analyzed in five distinct zones deviated by 1.5 mm each along an axial line of the surface. NRA and RBS sum spectra collected using incident 1000 keV, or 1000 keV and 2300 keV, $^3\text{He}^+$ beams) were analyzed simultaneously with the NDF code [18] to quantify the depth profiles of retained deuterium.

3. Results and discussion

3.1. Microstructural analysis

Fig. 1 displays the microstructures of CrNbTaVW and $\text{CrNbTaVW}_{1.7}$ HEAs before and after irradiation with one and three discharges observed in BSE mode. The microstructure of the non-irradiated CrNbTaVW sample (**Fig. 1(a)**) shows a fine eutectic mixture where each phase is smaller than 1 mm. After one discharge, the CrNbTaVW sample displays cracks through its surface (black arrow in **Fig. 1(c)**). Moreover, the microstructure also reveals the presence of blisters (white arrow in **Fig. 1(c)**), most of which are detached from a fully cracked surface. Looking at the sample with three discharges it is possible to see that it suffers the same type of damage observed in the previous one, with no visible morphological evolution. **Fig. 1(b)** shows a non-irradiated $\text{CrNbTaVW}_{1.7}$ sample with one major phase and two minor darker phases [13]. The sample irradiated with one discharge shows areas with swelling and some fissures on top of the swelling areas (see white arrow in **Fig. 1(d)**). The swelling observed on the $\text{CrNbTaVW}_{1.7}$ after three discharges appear to be more severe (see white arrow in **Fig. 1(f)**) when compared to the sample with one discharge. It is worth noticing that the increase in the number of discharges appears to promote the increase of swelling on the sample with higher tungsten content. Irradiation with D and He on tungsten at moderate temperature (<800 K) [2,19] resulted in blistering on the surface, while single He irradiation at higher temperature (>1600 K) [20] in tungsten leads to the formation of pits, holes, and bubbles. These features are associated with the accumulation of diffusing D and He in extended defects. Moreover, the observed irradiation swelling is caused by the irradiation-induced displacement of normally aligned lattice atoms from their original positions, resulting in the formation of vacancies and interstitials in the matrix [21,22] which reduces the material toughness which will seriously threaten the service life and safety of the reactors.

Fig. 2(a) to (f) shows the EDS map of the irradiated $\text{CrNbTaVW}_{1.7}$ sample. In spite of the severe swelling and melting observed, no changes in the surface composition were observed in the samples after irradiation. The EDS spectrum in **Fig. 2(g)** corresponds to the area presented in **Fig. 2(a)** to (f) and shows the presence of all the expected elements without any significant contamination. Similar results were observed in the EDS analysis of the second alloy.

3.2. Ion beam analysis

Fig. 3 evidences the results of NRA spectra collected during the experiment using 1000 keV (able to quantify deuterium down to 1.3 μm depth) and 2300 keV (able to quantify deuterium down to 3.3 μm) $^3\text{He}^+$ ion beams for both samples (CrNbTaVW and $\text{CrNbTaVW}_{1.7}$), together with the fit lines achieved for deuterium quantification using the NDF code [18]. **Table 3** shows the deuterium retention values based on the analysis of NRA spectra and using also NDF code. Comparing the results achieved from the superficial NRA analysis (performed only with 1000

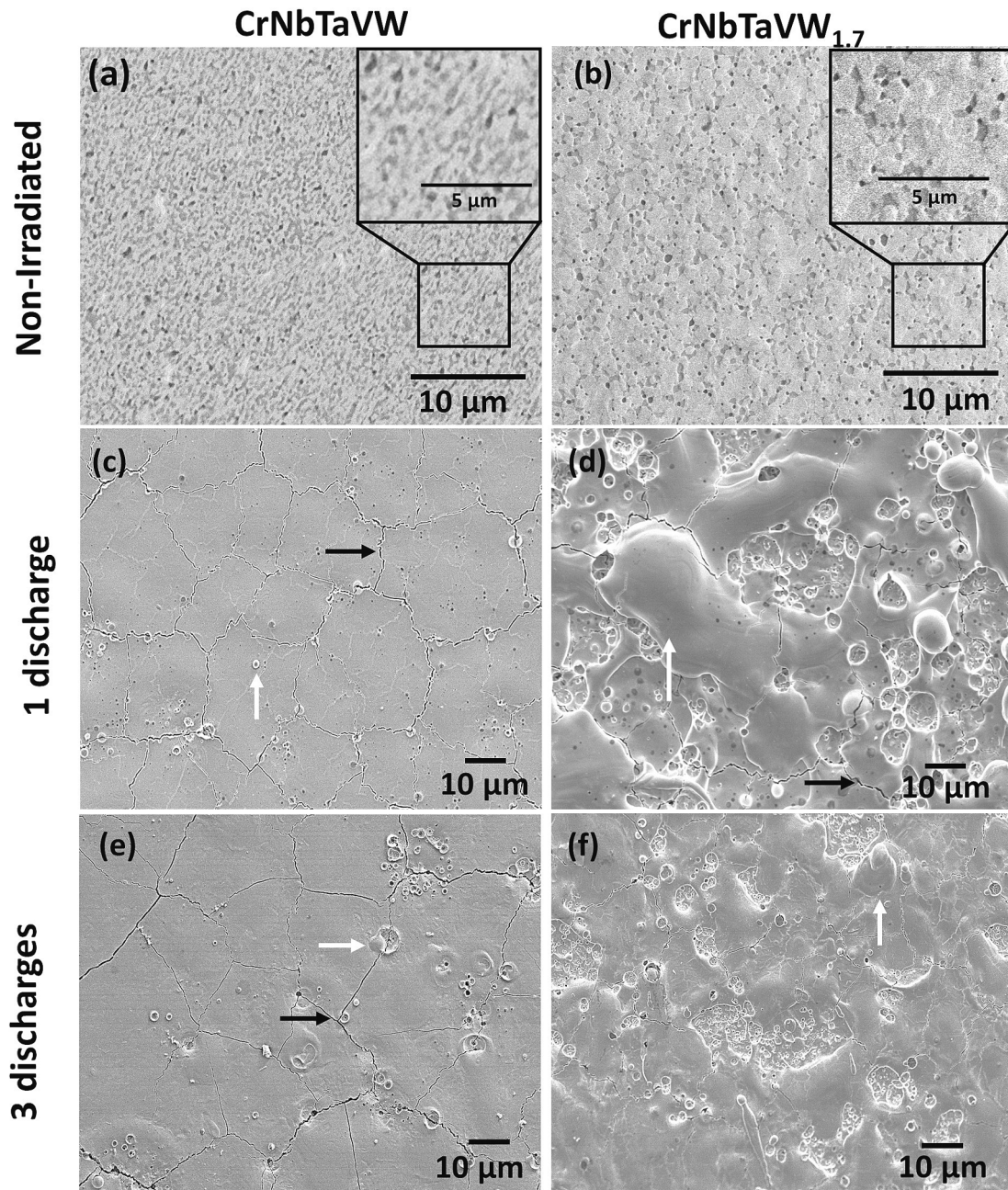


Fig. 1. SEM images showing the microstructures of (a), (c) and (e) are equiatomic CrNbTaVW and (b), (d) and (f) are CrNbTaVW_{1.7} high-entropy alloys and non-irradiated and irradiated with 1 and 3 discharges. The black arrows in (c) and (d) indicate the presence of the cracks in the surface. The white arrow in (c) shows blister, white arrow in (d) and (f) shows swelling.

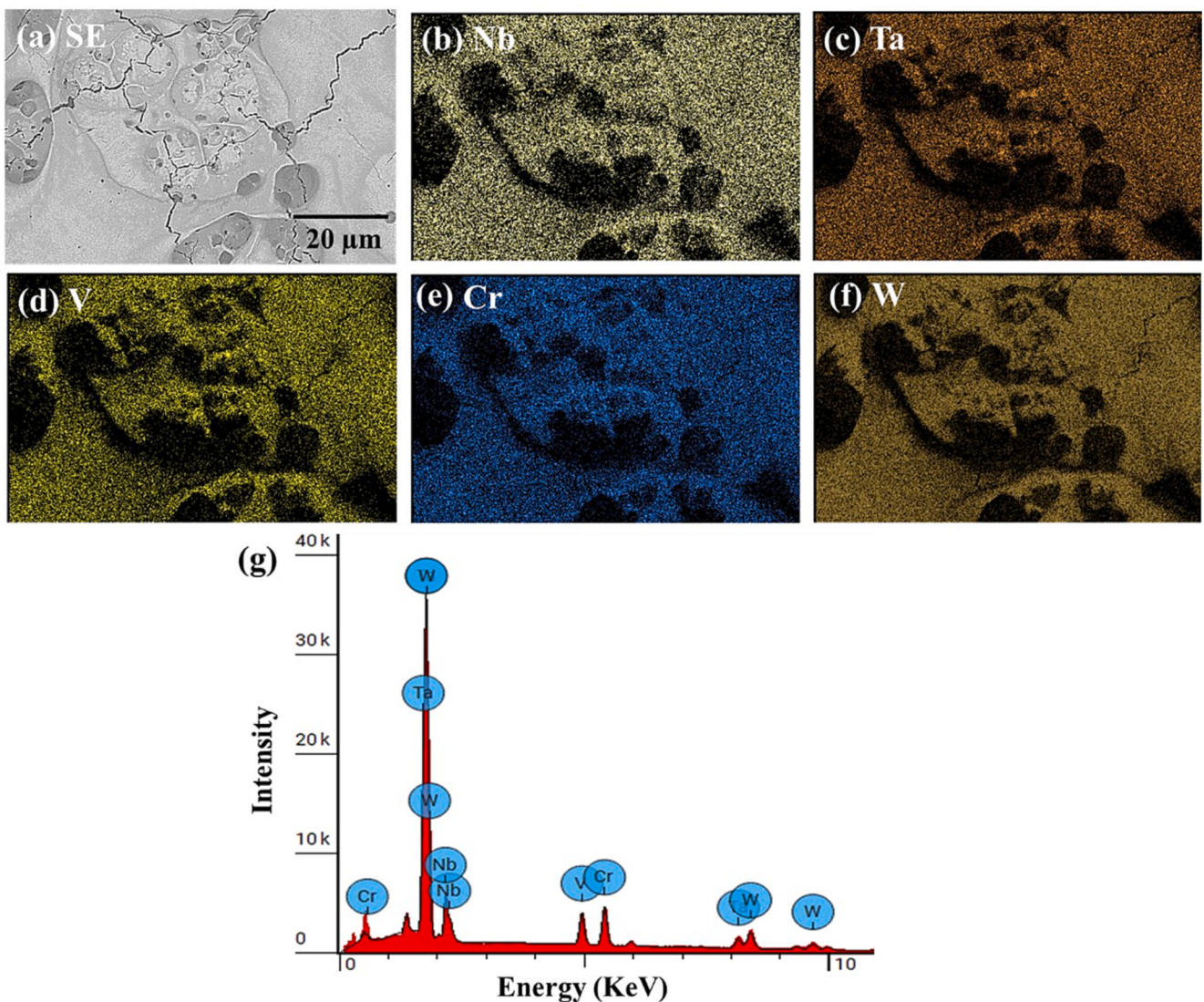


Fig. 2. SEM images and EDS map of CrNbTaVW_{1.7} sample irradiated with three discharges. (a) SE image, (b) Nb- L α , (c) Ta- L α , (d) V- L α , (e) Cr-L α , (f) W- L α X-ray lines respectively. Image (g) shows the EDS spectrum in area from SE image (a).

keV) and from the NRA analysis at deeper depths (performed simultaneous from both spectra collected at 1000 and 2300 keV) it can be observed that deuterium retention lies within a depth higher than 1.3 mm. Therefore, a higher amount of deuterium is retained between 1.3 and 3 mm in agreement with the graph showed in Fig. 3(e) which shows the deuterium retention as function of depth. This effect can be explained by the diffusivity of deuterium atoms to the bulk material caused by the heating of the targets associated with the heat flow during irradiation. The NRA yield for both samples is very similar (for one or three discharges) for the analysis at 1000 keV, however for the spectra collected at 2300 keV, the deuterium retention for three discharges is clearly higher.

Recent publications of deuterium retention on HEAs at high temperatures indicate that its retention mechanism is associated with the D trapping by the defects on the material which can increase the value of retention compared to pure W [23]. In addition, the different microstructures composition seems to be associated with the D retention. The sample with a eutectic microstructure (CrNbTaVW) evidences less D retention when compared with the swelling and blistering surface of the CrNbTaVW_{1.7}. It can be concluded that probably the phases presented on the eutectic structure (CrNbTaVW) can reduce less D when compared

with those in CrNbTaVW_{1.7}.

4. Conclusion

The CrNbTaVW and CrNbTaVW_{1.7} HEAs have been produced to work as potential plasma facing components in nuclear reactors. In this work, it was presented the analysis and characterization of irradiation on these materials. The effect of irradiation was more severe in CrNbTaVW_{1.7} when compared to CrNbTaVW, evidencing swelling in all the surface. Moreover, the deuterium retention was evidenced to be in a deeper depth between 1.3 and 3.3 μm and it was higher for the sample with higher W content. This phenomenon seems to be associated with trapping of D on the defects, however transmission electron microscopy is required to clarify this issue.

Declaration of Competing Interest

The authors declare that they have no known competing financial interests or personal relationships that could have appeared to influence the work reported in this paper.

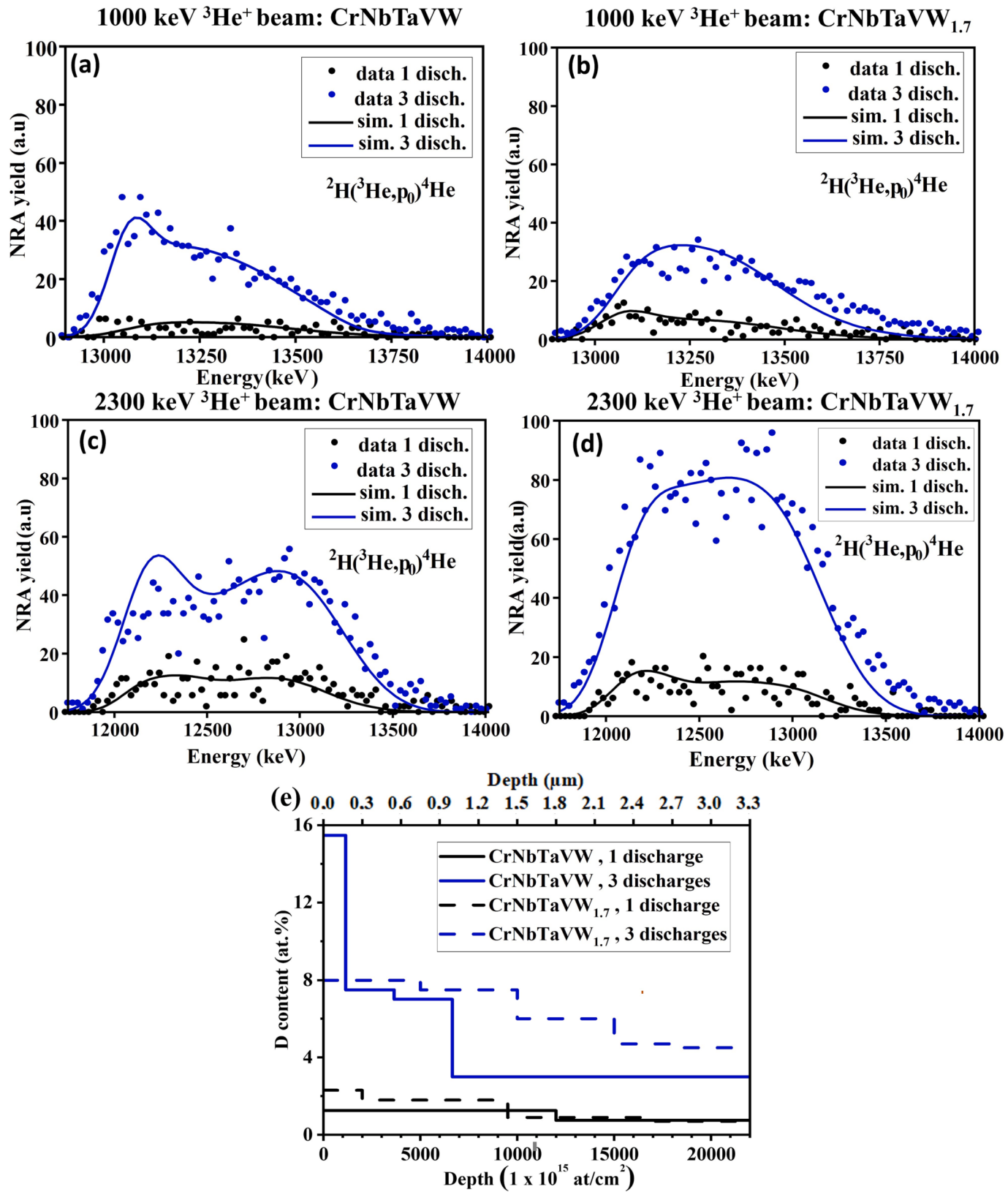


Fig. 3. Analysis of the as-irradiated CrNbTaVW and CrNbTaVW_{1.7} HEAs by NRA. (a) (b) are NRA measurement at 1000 keV and (c) and (d) are NRA measurement at 2300 keV. (e) D content“ vs “Depth for 1 and 3 discharges depth profiles of retained deuterium quantify via NDF code [18].

Table 3

Deuterium retention values after irradiation with 1 and 3 plasma discharges for the compositions CrNbTaVW and CrNbTaVW_{1.7}.

Sample	# discharges	Deuterium retention 1000 keV ³ He ⁺ (1 × 10 ¹⁵ cm ²)	Deuterium retention 2300 keV ³ He ⁺ (1 × 10 ¹⁵ cm ²)
CrNbTaVW	1	0.88	2.64
	3	8.89	10.60
CrNbTaVW _{1.7}	1	1.78	2.94
	3	7.92	13.90

Acknowledgments

The authors wish to thank to S. Glowacki, A. Arkuszewski, A. Szymaszek all the support in the PF-1000U operation and irradiation campaign. The present IPFN activity received financial support from “Fundação para a Ciência e a Tecnologia” through projects UID/FIS/50010/2020 and PTDC/FIS-PLA/31629/2017. IPFN and IFPiLM has also received funding from the “International Atomic Energy Agency” through CRP “Pathways to Energy from Inertial Fusion: Materials Research and Technology Development” (CRP 2250, Project code F13020) under the research agreement contracts 24119 and 24129.

References

- [1] W.D. Klopp, A review of chromium, molybdenum, and tungsten alloys, *J. Less-Common Met.* 42 (3) (1975) 261–278.
- [2] W.M. Shu, G.N. Luo, T. Yamanishi, Mechanisms of retention and blistering in near-surface region of tungsten exposed to high flux deuterium plasmas of tens of eV, *J. Nucl. Mater.* 367–370 B (SPEC. ISS.) (2007) 1463–1467.
- [3] O. El-Atwani, N. Li, M. Li, A. Devaraj, J.K.S. Baldwin, M.M. Schneider, D. Sobieraj, J.S. Wróbel, D. Nguyen-Manh, S.A. Maloy, E. Martinez, Outstanding radiation resistance of tungsten-based high-entropy alloys, *Sci. Adv.* 5 (3) (2019).
- [4] P. Gumbsch, Brittle fracture and the brittle-to-ductile transition of tungsten, *J. Nucl. Mater.* 323 (2–3) (2003) 304–312.
- [5] A.K. Sinha, V.K. Soni, R. Chandrakar, A. Kumar, Influence of refractory elements on mechanical properties of high entropy alloys, *Trans. Indian Inst. Met.* 74 (12) (2021) 2953–2966.
- [6] X. Hu, X. Liu, D. Yan, Z. Li, A high-density non-equiautomic WTaMoNbV high-entropy alloy: alloying behavior, microstructure and mechanical properties, *J. Alloys Compd.* 894 (2022), 162505.
- [7] C.-J. Tong, M.-R. Chen, J.-W. Yeh, S.-J. Lin, S.-K. Chen, T.-T. Shun, S.-Y. Chang, Mechanical performance of the AlxCrCuFeNi high-entropy alloy system with multiprincipal elements, *Mater. Trans. A Phys. Metall. Mater. Sci. Metall. Mater. Trans. A* 36 (5) (2005) 1263–1271.
- [8] H.P. Chou, Y.S. Chang, S.K. Chen, J.W. Yeh, Microstructure, thermophysical and electrical properties in AlxCrFeNi ($0 \leq x \leq 2$) high-entropy alloys, *Mater. Sci. Eng. B Solid-State Mater. Adv. Technol.* 163 (3) (2009) 184–189.
- [9] M.-H. Tsai, C.-W. Wang, C.-W. Tsai, W.-J. Shen, J.-W. Yeh, J.-Y. Gan, W.-W. Wu, Thermal stability and performance of NbSiTaTiZr high-entropy alloy barrier for copper metallization, *J. Electrochem. Soc.* 158 (11) (2011) H1161.
- [10] N.A.P.K. Kumar, C. Li, K.J. Leonard, H. Bei, S.J. Zinkle, Microstructural stability and mechanical behavior of FeNiMnCr high entropy alloy under ion irradiation, *Acta Mater.* 113 (2016) 230–244.
- [11] M. Moorehead, et al., High-throughput synthesis of Mo-Nb-Ta-W high-entropy alloys via additive manufacturing, *Mater. Des.* 187 (2020), 108358.
- [12] S. Zeng, Y. Zhu, W. Li, H. Zhang, H. Zhang, Z. Zhu, A single-phase Ti₃Zr_{1.5}NbVA_{10.25} refractory high entropy alloy with excellent combination of strength and toughness, *Mater. Lett.* 323 (May) (2022), 132548.
- [13] F. Antão, R. Martins, J.B. Correia, R.C. da Silva, A.P. Gonçalves, E. Tejado, J. Y. Pastor, E. Alves, M. Dias, Improvement of mechanical properties with non-equimolar CrNbTaVW high entropy alloy, *Crystals* 12 (2) (2022) 219.
- [14] K. Fujii, Precision density measurements of solid materials by hydrostatic weighing, *Meas. Sci. Technol.* 17 (10) (2006) 2551–2559.
- [15] V.A. Gribkov, I.V. Borovitskaya, E.V. Demina, E.E. Kazilin, S.V. Latyshev, S. A. Maslyaev, V.N. Pimenov, T. Laas, M. Paduch, S.V. Rogozhkin, Application of dense plasma focus devices and lasers in the radiation material sciences for the goals of inertial fusion beyond ignition, *Matter Radiation at Extremes* 5 (4) (2020) 045403.
- [16] M.S. Ladygina, E. Skladnik-Sadowska, D.R. Zaloga, M.J. Sadowski, M. Kubkowska, E. Kowalska-Strzeciwiłk, N. Krawczyk, M. Paduch, R. Miklaszewski, I.E. Garkusha, Studies of plasma interactions with tungsten targets in PF-1000U facility, *Nukleonika* 61 (2) (2016) 149–153.
- [17] M. Kubkowska, E. Skladnik-Sadowska, R. Kwiatkowski, K. Malinowski, E. Kowalska-Strzeciwiłk, M. Paduch, M.J. Sadowski, T. Pisarczyk, T. Chodukowski, Z. Kalinowska, E. Zielinska, M. Scholz, Investigation of interactions of intense plasma streams with tungsten and carbon fibre composite targets in the PF-1000 facility, *Phys. Scr. T161* (2014) 014038.
- [18] N.P. Barradas, C. Jeynes, R.P. Webb, Simulated annealing analysis of Rutherford backscattering data, *Appl. Phys. Lett.* 71 (2) (1997) 291–293.
- [19] S. Nagata, B. Tsuchiya, T. Sugawara, N. Ohtsu, T. Shikama, Helium and hydrogen trapping in W and Mo single-crystals irradiated by He ions, *J. Nucl. Mater.* 307–311 (2 SUPPL.) (2002) 1513–1516.
- [20] D. Nishijima, M.Y. Ye, N. Ohno, S. Takamura, Incident ion energy dependence of bubble formation on tungsten surface with low energy and high flux helium plasma irradiation, *J. Nucl. Mater.* 313–316 (SUPPL.) (2003) 97–101.
- [21] S.J. Zinkle, J.T. Busby, Structural materials for fission & fusion energy, *Mater. Today* 12 (11) (2009) 12–19.
- [22] S.J. Zinkle, G.S. Was, Materials challenges in nuclear energy, *Acta Mater.* 61 (3) (2013) 735–758.
- [23] Y. Shi, et al., Deuterium retention and desorption behavior of W-Ta-Cr-V high entropy alloy, *J. Nucl. Mater.* 568 (2022), 153897.